ISSN 0354-8724 (hard copy) | ISSN 1820-7138 (online)

When Ungauged Micro-Watersheds Conceal Danger: A Morphometric and Morphodynamic Analysis of Flood Risk. Case Study: The City of Aïn M'lila, Algeria

Nedjoua Cemali[A1], Sihem Ramoul[B]

Received: July 30, 2025| Revised: December 15, 2025| Accepted: December 16, 2025

doi: 10.5937/gp29-60528

Abstract

Extreme weather events-particularly episodes of intense rainfall-are increasingly disrupting hydrological regimes and triggering frequent, destructive floods, especially in urban environments. These floods have severe repercussions on populations, infrastructure, and economic activities. While large river basins are typically monitored and extensively studied, small ungauged urban catchments remain poorly documented despite their critical role in generating localized hydrological hazards. This study focuses on a small ungauged watershed located in Aïn M'lila (northeastern Algeria), which experiences recurrent flash floods that frequently lead to urban inundation. In the absence of hydrological instrumentation, the objective is to generate insight into the watershed's hydrological functioning and the associated geomorphological impacts using alternative, integrative methods. The approach combines morphometric analysis, a morphodynamic reading of surface flow dynamics, and targeted field observations of flood traces and erosion patterns. This methodological framework offers a more precise characterization of the watershed's specific features, enhances understanding of its behavior during extreme rainfall events, and provides a transferable basis for flood risk assessment in other similarly data-scarce urban contexts. This study contributes in three concrete ways: (1) by demonstrating a reproducible workflow that integrates 30 m DEM-based morphometry with field-scale morphodynamic observations for ungauged urban micro-watersheds; (2) by providing quantified morphometric metrics linked to hydrological response indicators (e.g., drainage density, time of concentration) and interpreting their physical meaning for flash-flood generation; and (3) by combining spatial evidence with participatory survey data to inform practical recommendations for low-cost monitoring and urban planning interventions.

Keywords: Floods; Small ungauged watersheds; Morphometric analysis; Morphodynamic interpretation; Flood risk; Urban environments; Aïn M'lila

1 Corresponding author: Nedjoua Cemali; e-mail: nedjoua.cemali@gmail.com

[A] Faculty of Earth Sciences and Architecture, Larbi Ben M'hidi University, Oum El Bouaghi, Algeria

[B] Faculty of Earth and Universe Sciences, Department of Geography and Spatial Planning, Moustapha Ben Boulaïd University, Batna, Algeria

Introduction

In developing countries, river basins play a strategic role in territorial planning and the management of water resources. Major basins -such as the Nile, Congo, and Niger in Africa-serve as natural units for water governance, often transcending administrative boundaries. These large-scale systems are essential pillars for irrigated agriculture, potable water supply, hydroelectric power generation, and ecosystem regulation.

At the same time, small sub-catchments-integral components of larger basins-are increasingly recognized for their importance in decentralized and participatory natural resource management. Their reduced scale allows for more precise integration of local specificities, particularly in relation to erosion control, flood mitigation, and water accessibility. This dual dynamic highlights the need to reconcile macro-scale planning with locally grounded interventions for effective water governance.

In the Mediterranean region, watersheds display distinct climatic and hydrological characteristics, including limited water resources, long dry summers, and high-intensity rainfall events that often trigger sudden floods (Merheb et al., 2016). Within this context, small catchments are especially sensitive hydro-geomorphological units (Seethapathi et al., 2008).

In recent years, flooding has become a central concern in debates on climate change impacts. Numerous studies have highlighted the intensification of extreme precipitation and the increasing frequency of flood events across various regions, particularly in the Mediterranean (Tramblay & Somot, 2018). In Algeria, the growing occurrence of extreme hydro-meteorological events has been accompanied by a steady increase in the availability of climatic and hydrological data, particularly for large, gauged basins. This wealth of data has sparked considerable scientific interest, as reflected in the extensive hydrological modeling literature by researchers such as Meddi, Bouanani, and Elahcene (e.g., Meddi et al., 2009; Achite, 2023; Elahcene, 2013).

However, this focus on well-documented catchments has contributed to the marginalization of small, ungauged watersheds, particularly those located on urban fringes or in neglected rural areas. Despite the absence of hydrometeorological time series, these basins are capable of generating intense hydrological responses, including flash floods that can inflict significant downstream damage. Their hydrological potential—exacerbated by the effects of climate change—remains significantly underestimated in risk management frameworks precisely due to the lack of available data.

Climate change further amplifies the vulnerability of small, ungauged catchments through both the intensification of extreme rainfall events (IPCC, 2021) and shifts in hydrological regimes (Özcan et al., 2025). In North Africa, climate projections for 2050 forecast an increase in the frequency and intensity of extreme precipitation directly linked to global warming (World Bank, 2020). In Tunisia, for instance, 100-year daily rainfall totals are projected to increase by approximately 20%. While the frequency of such events may decrease in Morocco and Algeria, their rising intensity significantly heightens flood risk (World Bank, 2020). These climatic shifts pose major threats to agricultural systems, infrastructure, and the sustainable management of water resources.

Despite the growing literature on well-instrumented basins, there remains a knowledge gap in how to generate actionable, quantitative flood-risk insight for small (<25 km^2), ungauged urban watersheds using accessible geospatial data and direct field evidence. This study aims to (i) quantify key morphometric indicators from a 30 m DEM and interpret their hydrological implications for flash-flood generation; (ii) integrate morphodynamic field evidence and a targeted participatory survey to validate flow paths and propose pragmatic risk-reduction measures.

This study aims to draw attention to the hydrological risks posed by small, ungauged watersheds risks that remain largely overlooked by local stakeholders and researchers due to data scarcity. Despite their capacity to generate substantial runoff during heavy rainfall events, these basins are still widely neglected in risk prevention and management strategies (Jakubínský et al., 2014).

Drawing on a rainfall event that occurred in June 2023 in the city of Aïn M'lila, this study employs a suite of accessible tools—including morphometric and morphodynamic analyses, slope and hydrography mapping, flood trace identification, and field photography. The objective is to transform fragmented data into structured and actionable knowledge. This research provides a foundation for further academic inquiry into small, data-scarce watersheds and aims to raise awareness among local decision-makers regarding their significance. Ultimately, it advocates for the integration of these overlooked hydrological systems into land-use planning and risk prevention policies.

Study Area

The watershed under investigation is located within the municipality of Aïn M'lila, which is administratively part of the Oum El Bouaghi province in northeastern Algeria. It is a small, ungauged catchment situated directly upstream of the urban area of

Aïn M'lila, contributing significantly to the city's flood exposure.

A land-cover classification performed on the Landsat (2024) image indicates that the basin comprises approximately: built-up/urban areas 48.32% (compact urban centre and expanding residential zones), green spaces/vegetation 39.71% (annual crops, gardens, and sparse vegetation), and bare soil 11.84%. This quantitative description highlights the significant extent of urbanization, which is central to understanding runoff generation in the basin.

The study area is characterized by a semi-arid Mediterranean climate, with marked seasonal and interannual variability in precipitation. Meteorological data from the Fourchi station (altitude Z = 775 m; coordinates X = 849.85, Y = 346.6) indicate a mean annual rainfall of 366.3 mm for the period 1976–2010, with significant fluctuations ranging from 187 mm in the driest years to 791.7 mm in exceptionally wet years. Winter and spring are the wettest seasons, receiving 115.12 mm and 116.23 mm, respectively, while the dry season occurs from June to August, with the lowest rainfall in June (6.11 mm). Other months with relatively low precipitation include September (36.4 mm), December (38.12 mm), and March (40.8 mm). Extreme events include daily rainfall reaching up to 125 mm, which is a major factor triggering flash floods in the micro-catchment.

This watershed functions as a tributary within the larger Oued Boumerzoug basin, of which it is a sub-affluent. Despite its modest surface area of 24.83 km², this micro-basin plays an active hydrological role-particularly during episodes of intense rainfall-when it serves as a conduit for rapid surface runoff toward the urbanized downstream zones (*see* Figure 1):

Data and Methodology

Urban streams are highly dependent on the hydrological behavior of their contributing catchments. As such, analyzing these upstream basins is an essential step in evaluating hydrological risks that may affect urban environments. In the present study, the case of the stream running through the city of Aïn M'lila is particularly illustrative, as it lacks both hydrometric and meteorological monitoring stations—making any attempt at data-driven hydrological analysis considerably more complex.

To address this limitation, the evaluation was based on a combined morphometric and morphodynamic analysis of the watershed. This integrated approach provides an initial understanding of the hydrological

Figure 1. Geographic location of the study area

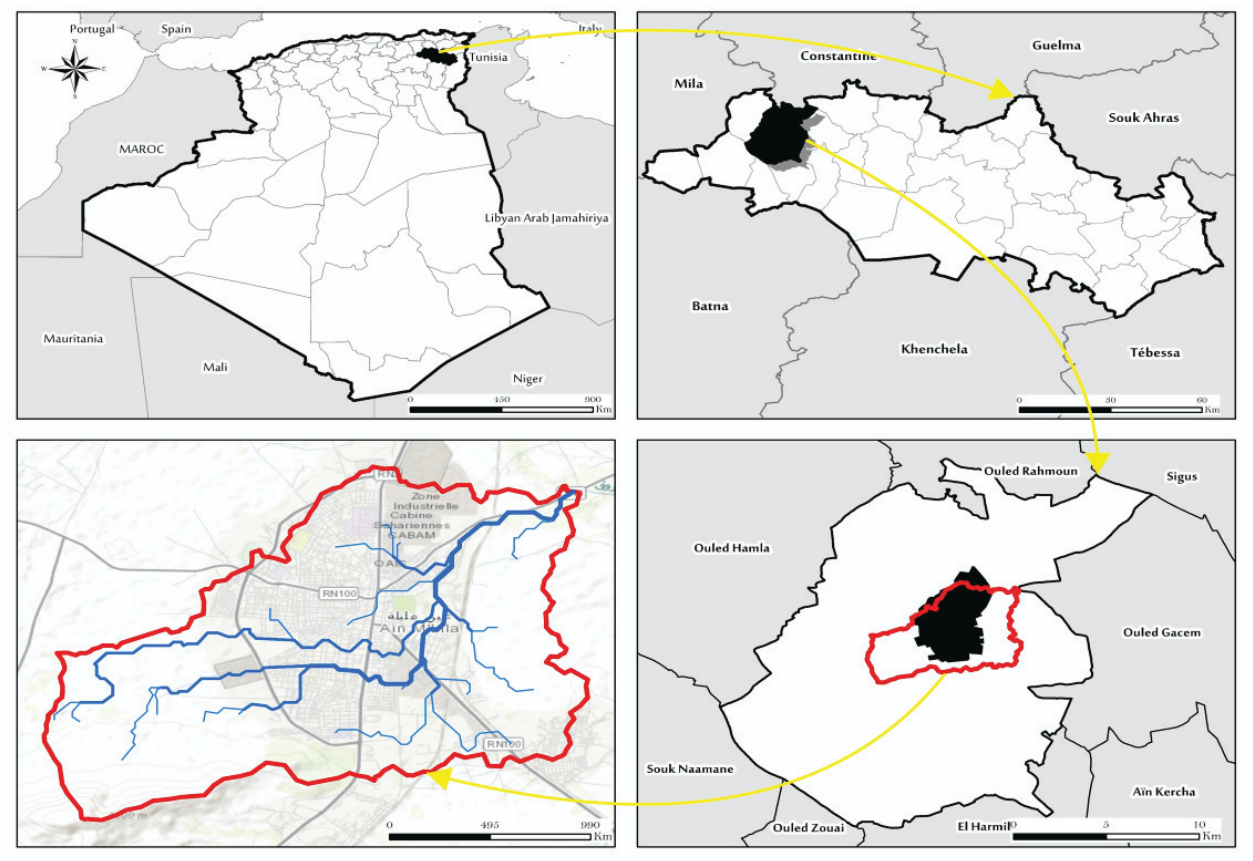

functioning and dynamic behavior of the studied urban micro-watershed.

The methodological framework adopted for assessing hydrological risk was structured into three complementary stages (*see* Figure 2):

Watershed Delineation and Morphometric Extraction

The watershed was delineated using a 30-meter resolution Digital Elevation Model (DEM) within ArcGIS 10.8. From this model, automated delineation of the catchment area was performed, and thematic maps were generated, including slope maps, elevation maps, and hydrographic network maps. Flow direction and flow accumulation were computed using the Hydrology tools of ArcGIS. A flow-accumulation threshold of 500 cells (45 hectares) or an alternative physical threshold of contributing area of approximately 0.45 km² was applied to extract the primary channel network in this micro-watershed. The threshold selection was tested sensibly by varying the accumulation threshold and visually validating network continuity against high-resolution satellite imagery and field-observed channels.

However, using a 30 m resolution DEM in the context of small urban catchments carries important limitations. A 30 m DEM is generally regarded as relatively coarse or medium resolution: the comparatively large cell size tends to smooth microtopographic variations, which can lead to under-detection of narrow thalwegs and to an overall simplification of the drainage network. This smoothing also causes a generalization of local slopes and curvatures, reducing the precision of derived slope, flow direction, and flow accumulation products; as a consequence, locations of flow convergence, overland flow paths, and small-scale connectivity can be misrepresented. For hydrological analyses in small urban basins—where microtopography and narrow channels strongly influence runoff concentration and flood routing—these effects can result in biased assessments of flow pathways and flood-prone areas, and therefore must be explicitly considered when interpreting results obtained from a 30 m DEM.

Morphometric Analysis

This step involved the calculation of several geometric, topographic, and hydrographic indices. These indicators allow for an indirect estimation of the

Figure 2. Schematic overview of the methodology used

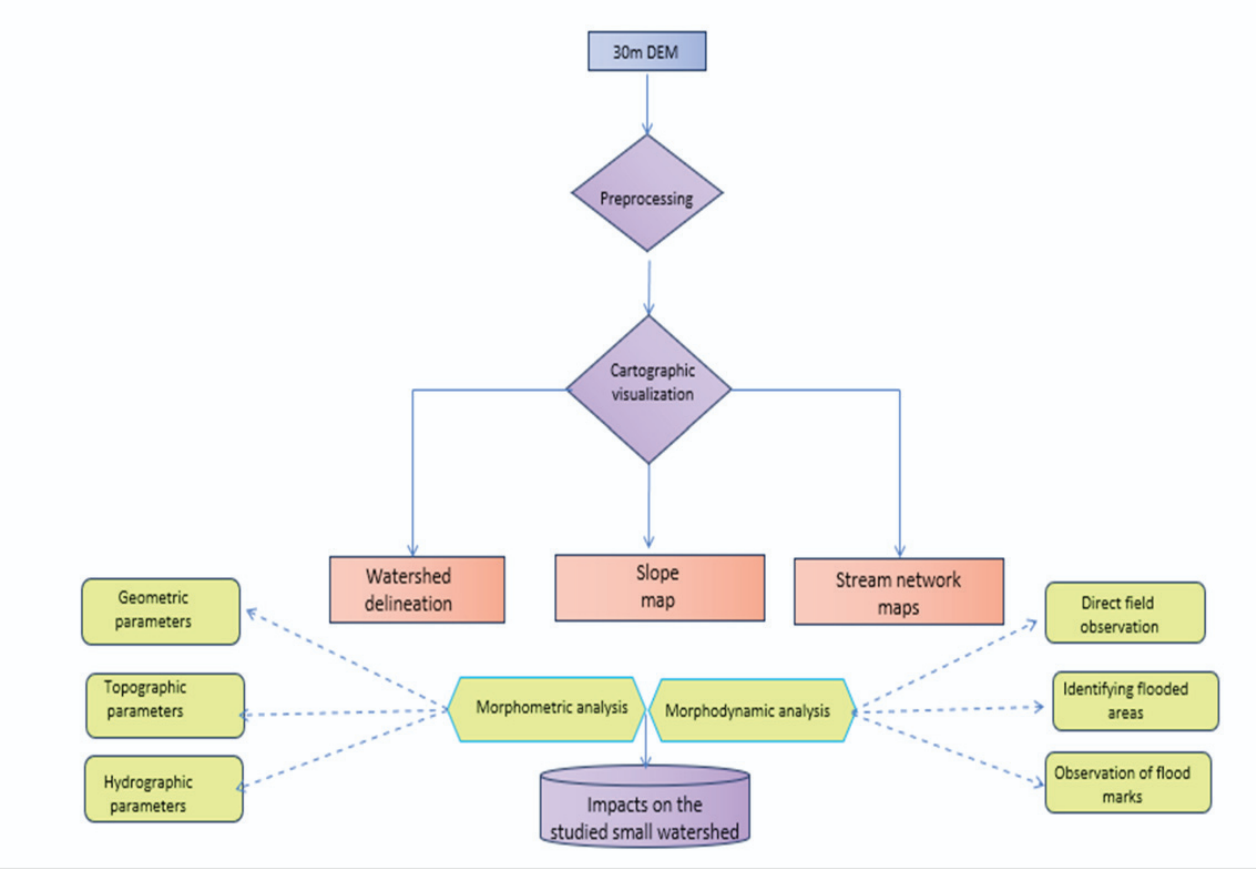

basin's hydrological responsiveness to intense rainfall events.

Morphodynamic Interpretation of a Flood Event and Participatory Survey

A field campaign was conducted in the most flood-affected areas, particularly in the Regaizi neighborhood. This phase involved identifying the main post-flood morphodynamic features—such as riverbank erosion, alluvial deposits, and alterations to the hydrographic network. Simultaneously, semi-structured interviews were conducted with local residents to document observed flood dynamics, perceptions of risk, and associated socio-economic impacts. This integrated approach made it possible to triangulate spatial data derived from remote sensing and GIS with empirical observations and local knowledge. To complement these observations, an exploratory survey was conducted with fifteen households along the main flow path to document the 2023 flood event. The survey focused on four themes: peak water heights inside and outside houses, frequency of past events, extent of damages, and perceived drivers of flooding. Qualitative data were analysed manually to identify recurring elements in respondents' statements. This survey aimed not at statistical representativeness, but at reconstructing flood characteristics through local knowledge.

The methodology was further enhanced by the use of a high-resolution satellite image from ALSAT-2, dated 2017 and obtained via the Algerian Space Agency (ASAL). This imagery made it possible to identify areas previously affected by flooding that correspond closely to the zones impacted during the June 2023 flood event. This spatial overlap supports the hypothesis of recurring extreme hydrological phenomena within the micro-watershed, despite the lack of long-term hydroclimatic data.

The integration of this satellite data strengthens the overall analytical framework by helping to locate areas that are frequently affected by flooding—an essential step in indirectly validating the watershed's hydrodynamic behavior.

Morphometric Analysis Method

Morphometric analysis constitutes a fundamental step in assessing the hydrological behavior of a watershed (Hamad, 2020), particularly in urban environments where dense development and soil impermeability intensify runoff processes. In the absence of continuous hydrometric data, morphometric analysis serves as a valuable proxy for understanding the watershed's response to extreme rainfall events (Garzon et al., 2023). This method enables a quantitative characterization of the basin's geometry, topography, and drainage network organization in order to identify the structural factors that influence surface runoff generation and concentration (Strahler, 1964; Horton, 1945).

Among the core hydrological parameters, watershed area is one of the most critical, as it directly determines the volume of surface water generated during a rainfall event. Under equal precipitation conditions, a larger drainage area implies a higher potential for runoff generation. This relationship is explicitly incorporated into the Rational Method, which is widely used to estimate peak discharge in small catchments, and it is a foundational component of various hydrological design methods applied to small basins (MFFP, 2018).

In this study, the watershed area was calculated using a 30-meter resolution Digital Elevation Model (DEM), employing ArcGIS Hydrology tools and following the method developed by Jenson and Domingue (1988). The catchment was delineated from the identified outlet by applying the *fill*, *flow direction*, and *flow accumulation* procedures.

In parallel with watershed delineation, several morphometric indices were calculated to characterize the basin's physical attributes. These parameters describe the basin's size, shape, topography, and the structure of its drainage network. They were derived from a 30-meter resolution DEM and a 1:50,000 scale topographic map.

The indices selected for this study are based on classical and widely accepted methodologies developed by Gravelius (1914), Horton (1945), Strahler (1957), among others. These indices are extensively used in contemporary scientific literature, particularly for evaluating watershed hydrological behavior (Shekar & Mathew, 2024). *Tables 1a and1b* presents the key morphometric indices employed, along with their respective formulas.

Morphodynamic Analysis Method

In ungauged watersheds—where no instrumental hydrological data (e.g., streamflow, water levels, or rainfall records) are available—post-flood morphodynamic analysis offers a valuable alternative for understanding surface flow dynamics. This method relies on the direct observation of the physical traces left by flood events, as well as the interpretation of runoff trajectories based on visual indicators and local testimonies. According to Alam and Ahmed (2020), when combined with topographic and spatial readings, morphodynamic observations can robustly reconstruct hydrological events—even in the absence of quantitative data. This approach is particularly well-suited to urban

Table 1a. Overview of the main geometric morphometric indices used.

	Index	Formula	Unit	Value	Reference
Geometric Parameters	Area of watershed	A	(km2)	24.83	Horton (1945)
	Perimeter of watershed	P	(Km)	25.54	
	Gravelius Compactness Index (KG)	$k_G = \frac{P}{2\sqrt{\pi A}} = 0.28 \times \frac{P}{\sqrt{A}}$		1.45	Gravelius (1914)
	Length/Width of Equivalent Rectangle (Lr / lr)	$\mathrm{Lr} = \frac{\mathrm{KG}\sqrt{\mathrm{S}}}{1{,}12} \times \left[1 + \sqrt{1 - \left(\frac{1{,}12}{\mathrm{G}}\right)^2}\right]$ $\mathrm{lr} = \frac{\mathrm{KG}\sqrt{\mathrm{S}}}{1{,}12} \times \left[1 - \sqrt{1 - \left(\frac{1{,}12}{\mathrm{G}}\right)^2}\right]$	(Km)	10.56 2.35	Benzougagh (2019)

Table 1b. Overview of the main topographic and hydrographic morphometric indices used.

	Index	Formula	Unit	Value	Reference
Topographic Parameters	Total Elevation Range (Dg)	$\mathrm{Dg} = \mathrm{H5\%} = \mathrm{H95\%}$	(m)	354	Benzougagh (2019)
	Minimum height	Hmax	(m)	1104	
	Maximum height	Hmin	(m)	750	
	Overall Slope Index (Ipg)	$\mathrm{Ipg} = \frac{\mathrm{D_g}}{\mathrm{Lr}}$		0.032	
Hydrographic Parameters	Drainage Density (Dd)	$\mathrm{Dd} = \frac{\sum_{i=1}^{n} \mathrm{L_i}}{\mathrm{s}}$	(km/km2)	1.41	Horton (1945)
	Time of Concentration (Tc)	$\mathrm{Tc} = \frac{4\sqrt{\mathrm{s}} + 1{,}5\mathrm{Lt}}{0{,}8\sqrt{\mathrm{H}}}$	(heures)	0.126h≈7.6min	Benzougagh (2019)
	Torrentiality Coefficient (Ct)	$\mathrm{Ct} = \mathrm{Dd} \times \mathrm{Fcl} = \mathrm{Dd}$		0.85	Mashauri (2023)

areas in developing contexts, where hazards are often underestimated due to the lack of instrumentation.

In the case of the Aïn M'lila watershed, the morphodynamic approach was implemented through a series of field observations conducted in the most severely affected zones. Key indicators included: submersion marks on walls and infrastructure (mud stains, waterlines), zones of concentrated erosion (at slope bases, along road edges, or on canalized banks), and sediment deposits (accumulations of gravel, ridges of fine materials, floating debris). These indicators allowed for the identification of runoff concentration zones and the localization of morphological impact points.

In addition to these observations, a participatory survey was carried out with local residents and shopkeepers. The semi-structured interviews helped validate hypotheses regarding water flow paths, clarify critical moments during the flood event (e.g., rate of water rise, duration of inundation), and provide insight into the flood's socio-spatial impacts (property damage, traffic disruptions, water intrusion into homes).

This methodological approach—rooted in the triangulation of visible flood traces, local perceptions, and fine-scale spatial interpretation—compensates for the lack of hydrological measurement and offers a meaningful understanding of runoff processes in uninstrumented urban environments. The integration of morphometric data, morphodynamic indicators, and GIS-based cartographic outputs enables a comprehensive interpretation of the ungauged micro-watershed's behavior during the flood event.

In the morphodynamic section, our observations drew on the concepts and examples set out by Bravard and Petts (2005), whose work offers clear, detailed insights into channel dynamics, the transfer of sediment during floods, and the identification of key geomorphic indicators — notably bank erosion, depositional forms, and channel adjustments.

Results and Discussion

The results of the morphometric and morphodynamic analyses provide a detailed reading of runoff processes within the watershed and allow for the identification of hydro-geomorphological susceptibility zones associated with the recent flood event. In a context characterized by the absence of instrumental hydrological data, the use of a Digital Elevation Model (DEM) enabled the generation of several key thematic maps, including slope maps, hypsometric (elevation) maps, and drainage network maps. These geospatial outputs form an essential analytical foundation for interpreting the hydrological and morphodynamic functioning of the basin.

This section presents a structured account of the main findings from spatial modeling, field observations on erosion dynamics and post-flood sediment deposits, and qualitative insights drawn from testimonies of residents directly affected by the event.

Topographic Interpretation of the Basin: Relief, Slopes, and Drainage Dynamics

As shown in **Figure 3,** the studied micro-watershed displays a pronounced altitudinal structure, with a gradual decrease in elevation from upstream to downstream. The highest point, located in the southwest, reaches 1,104 meters, while the outlet in the northeast lies at 757 meters—yielding a total elevation drop of 347 meters. Given the basin's modest area of 24.83 km², this altitudinal variation reflects a markedly contrasted topographic configuration. The spatial distribution of elevation suggests a structured gravitational runoff pattern oriented predominantly from the southwest to the northeast, which promotes rapid surface water concentration.

The slope map reveals a concentration of steep slopes (ranging from 9% to 40%) in the southwestern upstream section of the basin. This zone accounts for approximately 20% of the total basin area, while the remaining 80% is characterized by low slopes (less than 3%), mainly located in the midstream and downstream sectors (Figure 4). These lower-gradient areas—when combined with the presence of impervious surfaces in the downstream zones—facilitate rapid surface runoff, reduced infiltration, and a very short hydrological response time (Lei et al., 2020).

The dominant flow direction aligns with the basin's altitudinal gradient, running from the southwest to the northeast, consistent with the natural drainage pattern. In this context, the gently sloped downstream areas—particularly within the densely urbanized sections of old Aïn M'lila—serve as preferential zones for flow accumulation and water pooling, thereby increasing the risk of localized flooding.

Morphometric Interpretation of the Micro-Watershed

The morphometric analysis of the studied micro-watershed is based on a combined evaluation of geometric, topographic, and hydrographic parameters (*Tables 1a and 1b*). The computed geometric indicators—including area, perimeter, Gravelius compactness index, and equivalent length and width—point to a predisposition for hydrological sensitivity to rainfall inputs.

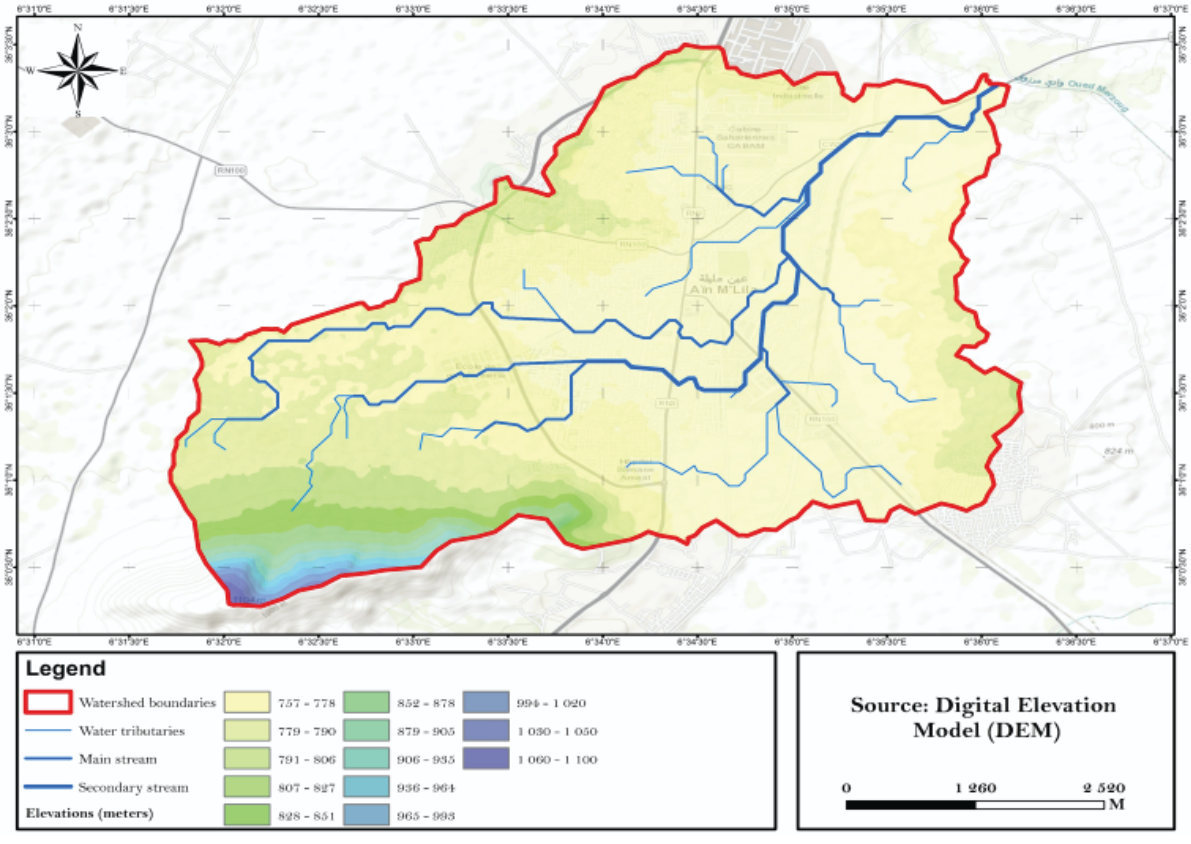

Figure 3. Altitudinal distribution of the studied micro-watershed

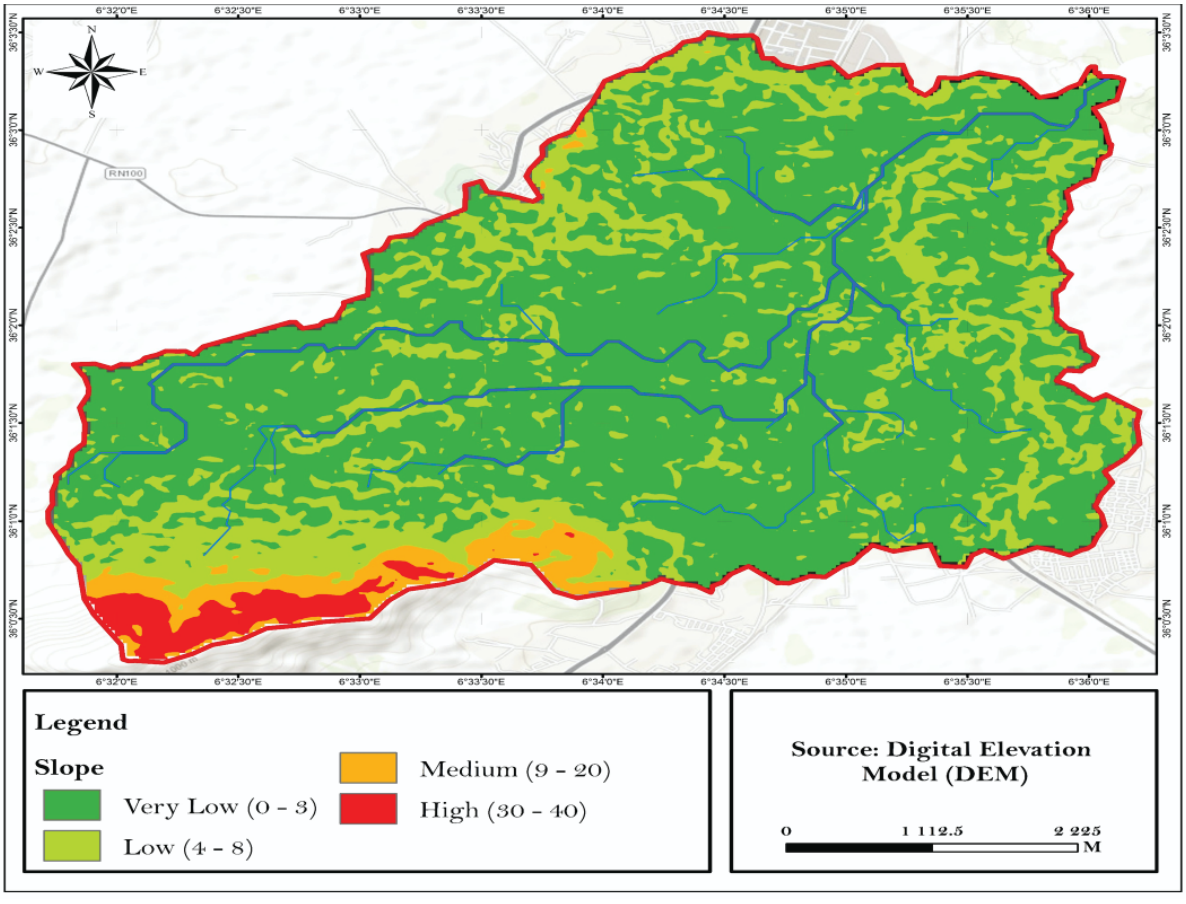

Figure 4. Slope distribution within the studied micro-watershed

For example, when the compactness index is greater than 1.12, it indicates that the catchment has an elongated shape (here Kg = 1.45). In theory, this type of shape leads to a slower concentration of runoff: the water takes longer to reach the outlet, resulting in a more gradual rise in floodwaters (Strahler, 1957). This relationship is consistent with flood hydrograph theory and shape-related morphometric controls. In general, elongated catchments, characterized by low shape indices, produce hydrographs spread out over time and relatively moderate flood peaks (Horton, 1945).

However, in the case of the studied basin, this morphometric organization does not result in a slow hydrological response. Despite its elongated shape (Kg = 1.45), the basin exhibits a rapid reaction to rainfall events. According to Strahler (1957) and Horton (1945), a drainage density greater than 1 km/km² indicates a well-developed hydrographic network, promoting rapid concentration and strong synchronization of flows. This configuration leads to a sharp rise in the hydrograph and a significant increase in peak discharge. In this context, the combined effect of a high drainage density and a very short time of concentration directly controls the scaling of peak flow at the outlet, overriding the moderating influence of basin elongation. The estimated time of concentration (Tc = 0.126 h, or approximately 7.6 minutes) thus confirms the occurrence of an early flood peak, appearing in the very first minutes following the rainfall event. The high drainage density (Dd = 1.41 km/km²) highlights a morphology particularly conducive to rapid water concentration and a high potential for flash floods, which helps to explain, at least in part, the flooding observed in the studied basin.

The analysis of topographic parameters provides additional insight into the basin's hydrological behavior. As shown in Table 1, the overall slope index reaches 3.2%, a value often cited (Strahler, 1957) as a limiting factor for flow concentration. However, the significant elevation difference of 354 meters indicates a varied topography that may generate locally elevated runoff velocities. This heterogeneity is confirmed by the spatial analysis of slope and elevation patterns (Figures 3 and 4).

The morphological interpretation is corroborated by a torrentiality coefficient of 0.85 (Table 1b). This coefficient reflects the basin's capacity to generate rapid, concentrated runoff during intense rainfall events, and values exceeding 0.7 are commonly associated with high torrential behavior. Consequently, the Ct value obtained indicates pronounced torrential dynamics and a strong hydrological reactivity of the watershed. When combined with the very short time of concentration (Tc = 0.126 h) and steep upstream slopes, this high torrentiality enhances runoff velocities, limits infiltration, and further amplifies peak discharge. These factors collectively increase the watershed's susceptibility to fast, high-magnitude flood responses and thus elevate its flood hazard potential.

When compared with other Mediterranean and semi-arid catchments, the rapid hydrological response observed in the study basin is consistent with similar findings. Morphometric analyses in the Wadi Easal Basin in Jordan (Obeidat et al., 2021) and the Oued Adoudou Basin in Morocco (Nait-Si et al., 2025) show that steep slopes, high relief, and dense drainage networks favor rapid runoff generation and high flood susceptibility. These studies support the interpretation of the present results within the broader context of Mediterranean and semi-arid environments.

Morphodynamic Response of the Watershed to the June 2023 Flood: Effects at the Basin and Urban Scales in Aïn M'lila

In the absence of monitoring stations or detailed hydrological data, direct field observation becomes an essential tool for understanding the dynamics of the June 2023 flood. Visible signs of erosion, sediment deposition, overflow, and gully formation—recorded during field surveys—provide valuable insights into the actual behavior of the watershed and the downstream urban runoff.

Visual analysis, supported by targeted photographic documentation, made it possible to reconstruct the flow paths and identify the sectors most exposed to hydro-geomorphological hazards.

Upstream Zone: Initial Flow Concentration

In the upstream portion of the basin, topographic configuration plays a decisive role in triggering surface runoff. During the June 2023 flood event, field observations revealed evidence of linear erosion, gully formation, and sediment accumulation in steep slope areas and along unpaved pathways. These features indicate early-stage flow concentration zones, where rainwater rapidly converged to form channelized flows.

Figure 5 illustrates two types of concentrated erosion forms observed at the headwaters of the basin. These features occur in areas characterized by steep gradients, sparse vegetation cover, and clearly visible water pathways—marking the onset of concentrated surface flow toward the downstream zones.

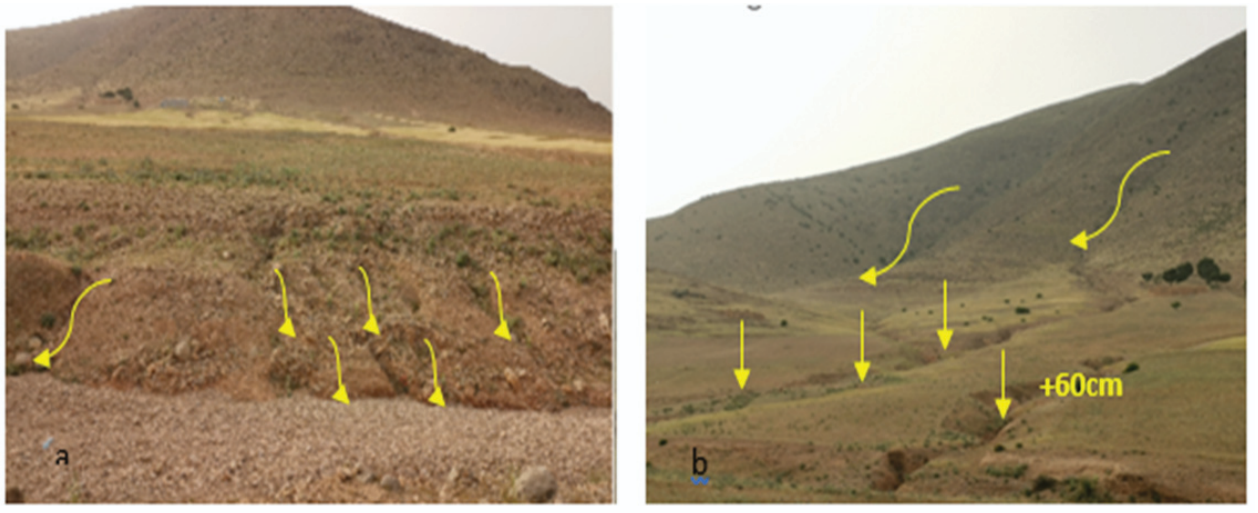

Figure 5. Signs of concentrated runoff on sloped terrain in the upstream zone of the watershed.
(a) Rill erosion caused by concentrated rainfall runoff on bare soil.
(b) Gully formation on an unvegetated slope, indicating active erosion processes during the June 2023 flood.

Intermediate Flow Path: Runoff Dynamics and Nature of Sediment Deposits

In the intermediate zone of the basin, flow paths were reconstructed through the analysis of sediment deposits left in the aftermath of the flood. These deposits—characterized by their grain size, thickness, and spatial distribution—enabled the tracing of runoff trajectories. Rills measured between 1.5 and 4 m in length and 0.1–0.3 m in depth, providing quantitative markers of concentrated flow paths. The sediment patterns reflect local variations in flow energy, indicating zones of intense concentration, decantation, or overflow.

The observed deposits exhibited clear granulometric sorting, with coarse materials (boulders and gravel, 50–200 mm in diameter) located within active channels and finer silts (0.05–0.2 mm) along channel banks and in adjacent agricultural plots. Estimated sediment volumes ranged from 0.5 to 2 m^3 per linear meter of channel, highlighting the considerable material transport during the flood.

This spatial distribution mirrors the underlying runoff dynamics: linear and uniform deposits indicate concentrated flow and high transport capacity, while diffuse and irregular deposits mark overflow areas and zones where flow energy gradually dissipated (Figure 6).

In specific areas of the basin, particularly near flow convergence zones, very thick sediment deposits—ranging from 1.5 to 3 m in thickness—were observed. These deposits were composed of coarse materials such as boulders, cobbles, and gravel. Their presence indicates that the flood event was not merely a case of superficial water runoff; rather, it involved highly sediment-laden flows.

Downstream from these zones of hydrodynamic concentration, homogeneous silty deposits mark a post-flood decantation phase, consistent with classical models of sedimentation under low-energy conditions. Approximately 15–20 % of the watershed area

Figure 6. Evidence of post-flood hydro-sedimentary dynamics in the intermediate zone of the watershed. (a, b) Main transport channel with coarse deposits (gravel and boulders), indicating strong post-flood flow concentration. (c) Branches deposited in the riverbed following the flood. (d) Erosion rills (20 to 50 cm deep) formed on an agricultural plot, reflecting localized overflow and temporary concentration of hydrodynamic energy.

exceeded critical slope thresholds (15–25 %), contributing to rapid runoff concentration and sediment transport. The uniform grain size and spatial distribution of these deposits reflect a gradual dissipation of flow energy—a phenomenon well-documented in fluvial systems subject to rapid flood events. This type of hydrodynamic behavior is extensively described in the work of Bravard (2000).

Downstream Zone: Limitations of Hydraulic Infrastructure and Vulnerability of Built Systems

Downstream of the hydrodynamic concentration zones, homogeneous silty deposits provide evidence of a post-flood decantation phase, in line with classical sedimentation models under low-energy flow regimes. The uniform grain size and spatial spread of these deposits reflect the progressive dissipation of flow energy—a phenomenon well documented in fluvial systems experiencing rapid flood events (Bravard, 2000).

This hydrodynamic slowdown is further confirmed by field observations, including the formation of stagnant water ponds—either clear or rich in algal blooms—within agricultural plots and anthropogenic depressions. These water bodies, resulting directly from the flood, reflect the inability of the flow to fully evacuate residual water, indicating both weak topographic constraints and insufficient flow energy for effective drainage (**Figure 7**).

The hydraulic infrastructure within the valley exhibits significant structural weaknesses in the face of extreme flood events, primarily due to design approaches that do not align with the actual morphometric and hydrological characteristics of the basin. These structures become quickly obstructed by transported debris, drastically reducing their operational capacity. Meanwhile, rigid linings and reinforcements fail under hydraulic overload, posing risks to the stability of roadways and adjacent infrastructure.

Figure 7. Post-flood stagnant water in the downstream zone: (a, b) Ponds formed in low-lying agricultural land. (c) Stagnant water in an anthropogenic depression within an urbanized area.

The drainage network is heavily impaired by sediment deposits and a lack of maintenance. Major transport corridors—such as the railway and National Road RN3—create topographic discontinuities that obstruct natural water flow, resulting in localized accumulation zones. Furthermore, the main stormwater drainage channel is under-designed both in slope and depth, severely limiting its functionality during high-flow periods (Figure 8).

Figure 8. Malfunctioning of the urban drainage system observed in the field: (a) Heavily loaded discharge canal, impairing proper flow. (b) Sewer blocked by solid waste, observed in a residential neighborhood. (c) Drainage structure clogged with poorly sorted coarse sediment deposits (silt, gravel), hindering flow and promoting overflow.

The drainage network suffers from poor maintenance, with frequent obstructions caused by debris and silty deposits. Both the railway line and National Road RN3 create artificial topographic barriers that trap water and exacerbate local accumulation. Even the main stormwater drainage canal—despite its 2000 mm diameter—has an insufficient slope, which severely compromises its evacuation capacity during flood events (Figure 9).

To enhance understanding of sediment dynamics within the watershed, a sediment transport map was developed (Figure 10) that delineates dominant flow pathways across the upper, middle, and lower sectors of the basin. This map identifies zones of preferential erosion, sediment transfer, and deposition, thereby establishing a coherent linkage between basin-scale morphodynamic processes and the localized impacts documented during flood events.

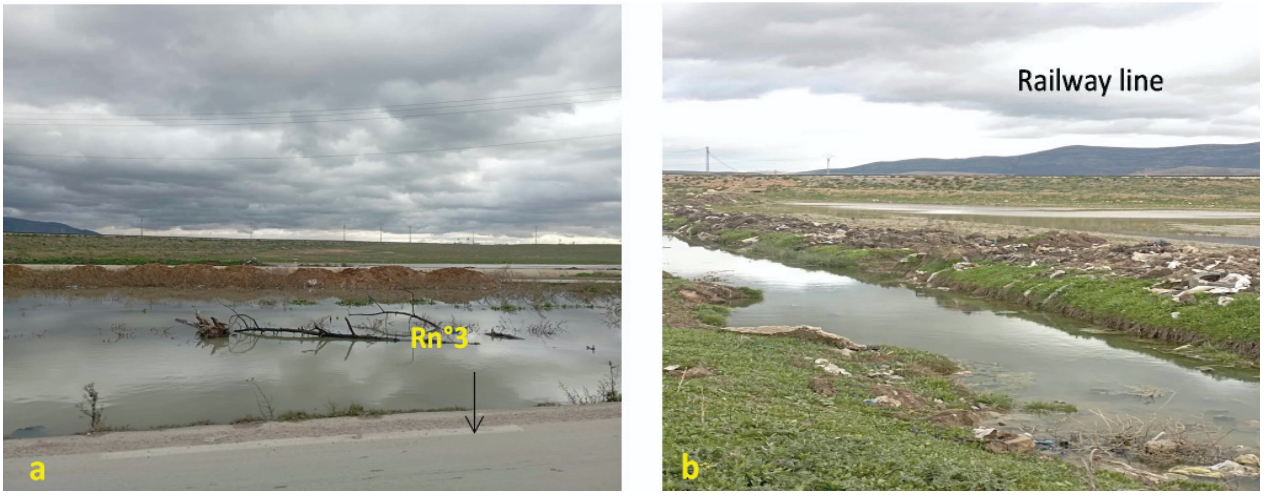

Figure 9. Water accumulation upstream of the railway line acting as a topographic barrier:
(a) Flooding of National Road RN3. (b) Accumulation of rainwater upstream of the railway due to the absence of adequate hydraulic crossings.

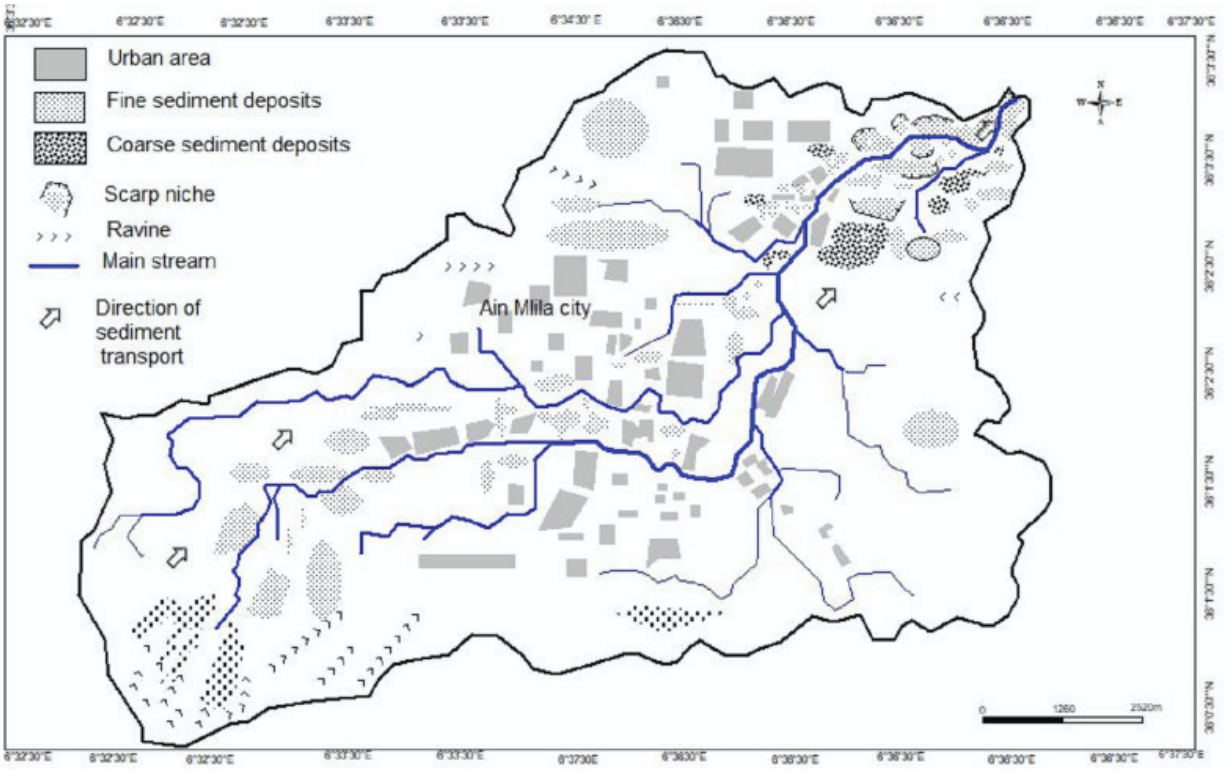

Figure 10. Spatial Distribution of Sediment Transport in the Watershed

In response to these observations, measurements were taken on the exterior walls of several homes located in low-lying areas along the watercourse, recording floodwater marks to estimate the maximum height reached by the waters. This assessment was supplemented by the analysis of photographs captured during the event, offering direct visual evidence of the flood's extent and severity (Figure 12). In addition, conversations with local residents helped reveal spontaneous forms of adaptation in the face of recurrent risk: raising door thresholds, installing gates or barriers, modifying building façades, and constructing small staircases to prevent water intrusion into living spaces. These resident-led interventions reflect both the recurring nature of flooding in the area and the glaring absence of a formal risk management strategy—even in recently built urban neighborhoods (Figure 11).

Figure 11. Effects of the June 2023 flood on buildings and residents' individual adaptations:
(a, b) Flood marks visible on the walls of a dwelling (June 2023). (c) Raised doorway threshold installed to limit water intrusion.

Figure 12. Submersion of residential neighborhoods during the June 2023 flood:
(a, b) Newly urbanized collective residential area. (c) Single-family home in an older neighborhood, inundated by floodwaters.

To deepen the morphodynamic analysis, a spatial verification was conducted using a high-resolution satellite image (ALSAT-2, 2017), provided by the Algerian Space Agency. This image highlights areas that have historically been affected by flooding within the study region.

By overlaying the flood zones identified in 2017 with the watershed boundary mapped on Google Earth imagery and its associated hydrographic network, it was observed that all sites impacted by the June 2023 flood are located within the same basin. This spatial coincidence reinforces the hypothesis of recurring extreme hydrological events, particularly in the lower reaches of the valley (Figure 13). This integration of satellite data, cartographic outputs, and field observations compensates for the absence of precise hydroclimatic records by offering a spatial validation of flood risk. It also underscores the necessity of adopting a systemic interpretation of the watershed, where any morphological disruption or change in land use can amplify the impacts of future flood events.

Nevertheless, several sources of uncertainty and methodological limitation must be acknowledged. The use of a 30 m resolution DEM may attenuate fine-scale

topographic variability, thereby influencing the accuracy of slope estimates, flow-path delineation, and the representation of micro-channel features. In the absence of direct hydrological measurements, analyses in this ungauged basin necessarily rely on indirect inferences of runoff and flow behavior. Moreover, the visual identification of flood traces and depositional forms involves an element of subjectivity, and some topographic or land-use datasets may not fully capture current surface conditions. The analysis is also grounded primarily in a single documented flood event, which constrains the extent to which the findings can be generalized to other hydrological scenarios. Despite these limitations, the integrative framework that combines morphometric analysis, targeted field observations, and GIS-based interpretation yields robust and informative insights into the basin's morphodynamic functioning.

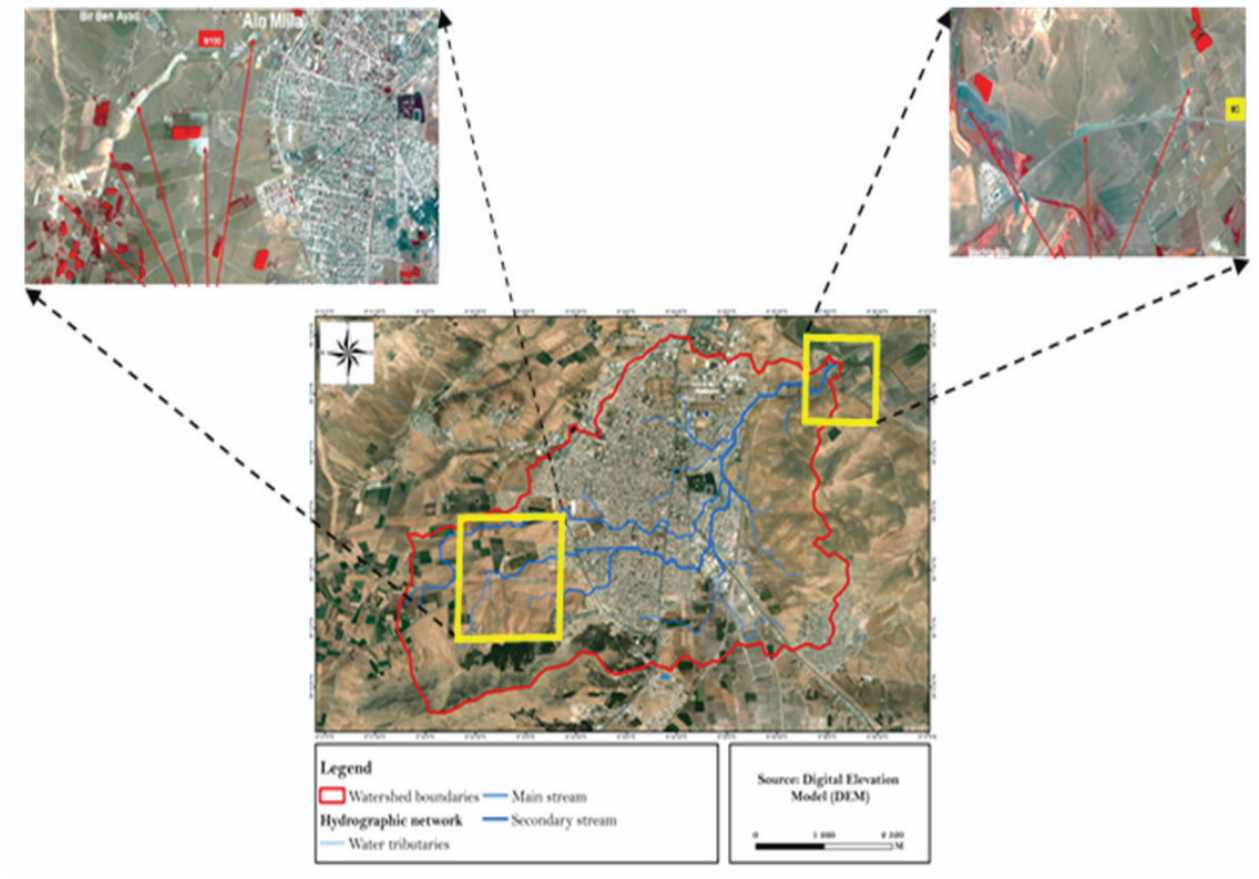

Figure 13. Identification of flood-prone areas within the studied watershed based on an ALSAT-2A satellite image with 2.5 m resolution, dated June 3, 2017.

Conclusion

This study elucidates the hydrological behavior of an ungauged micro-watershed responsible for localized flooding in Aïn M'lila during the June 2023 event. By integrating morphometric analysis, direct field-based observation of morphodynamic responses, and the cross-analysis of slope and hydrographic maps, the research provides refined insights into runoff processes and spatial vulnerability. It demonstrates that small, frequently overlooked watersheds can exert a disproportionate influence on the occurrence and severity of localized flood events.

In the absence of direct hydrological monitoring, the combined use of a Digital Elevation Model (DEM), slope analysis, and morphometric indicators proved critical for delineating the watershed, characterizing its topographic controls, and identifying zones susceptible to runoff concentration. The integration of these datasets with field evidence enabled the identification of sediment accumulation areas, overflow signatures, active erosion zones, and ephemeral flow pathways. In particular, neighborhoods such as Rezaigui were identified as highly vulnerable due to their downstream position relative to steep upstream slopes and their location within a diffuse hydrographic network, where rapid runoff concentration—enhanced by re-current convective rainfall—resulted in localized yet substantial damage.

These findings are consistent with assessments conducted by the Algerian Space Agency (ASAL), which, following the July 2017 flood, had already classified the same sectors as highly exposed using high-resolution ALSAT-2 satellite imagery. The recurrence of flooding in these areas underscores their pronounced vulnerability and highlights the urgency of integrating them into targeted and sustained flood risk prevention strategies.

From an applied perspective, the results emphasize the necessity for regular maintenance of urban drainage networks, the explicit consideration of sediment transport processes in land-use and urban planning, and the implementation of localized mitigation measures, such as retention basins or flow-attenuation structures. In addition, early warning systems adapted to the scale of micro-watersheds could substantially reduce exposure and damage in these high-risk zones.

More broadly, this study underscores the scientific and operational value of coupling spatial analyses with empirical field observations in small, ungauged watersheds. Future research should prioritize the deployment of low-cost hydrological monitoring devices to generate continuous runoff and sediment datasets, thereby supporting more robust risk assessments and the development of effective, integrated watershed management strategies.

Acknowledgements

The authors gra tefully acknowledge Dr. Benhamlaoui. A, for his assistance with the English language editin g of the manuscript and Mr A. Bouchachoua for his support during the fieldwork.

References

Achite, M., Katipoğlu, O. M., Jehanzaib, M., Elshaboury, N., Kartal, V., & Ali, S. (2023). Hydrological drought prediction based on hybrid extreme learning machine: Wadi Mina Basin Case Study, Algeria. *Atmosphere*, *14*(9), 1447. https://doi.org/10.3390/atmos14091447

Alam, A., Ahmed, B., & Sammonds, P. (2021). Flash flood susceptibility assessment using the parameters of drainage basin morphometry in SE Bangladesh. *Quaternary International, 575*, 295–307. https://doi.org/10.1016/j.quaint.2020.04.047

Benzougagh, B., Dridri, A., Boudad, L., Sdkaoui, D., & Baamar, B. (2019). Apport des SIG et télédétection pour l'évaluation des caractéristiques physiques du bassin versant d'oued Inaouene (Nord-Est Maroc) et leurs utilités dans le domaine de la gestion des risques naturels. *American Journal of Innovative Research and Applied Sciences, 8*(4), 120–130.

Bouchachou, A. (2023). *Morphodynamic reading of hydrological risks in small urban catchments: The case of Ain M'lila (Algeria)* (Master's thesis, University of Larbi Ben M'hidi, Oum El Bouaghi).

Bravard, J. P., & Petit, F. (2000). *Les cours d'eau : Dynamique du système fluvial*. Collection U.

Elahcene, O., Terfous, A., Remini, B., Ghenaim, A., & Poulet, J. B. (2013). Etude de la dynamique sédimentaire dans le bassin versant de l'Oued Bellah (Algérie). *Hydrological Sciences Journal*, *58*(1), 224–236.10.1080/02626667.2012.742530

Garzon, L. F. L., Johnson, M. F., Mount, N., & Gomez, H. (2023). Exploring the effects of catchment morphometry on overland flow response to extreme rainfall using a 2D hydraulic-hydrological model (IBER). *Journal of Hydrology, 627*, 130405. https://doi.org/10.1016/j.jhydrol.2023.130405

Ghaleno, M. R. D., Meshram, S. G., & Alvandi, E. (2020). Pragmatic approach for prioritization of flood and sedimentation hazard potential of watersheds. *Soft Computing, 24*(20), 15701–15714. https://doi.org/10.1007/s00500-020-04899-4

Gravelius, H. (1914). *Grundriß der gesamten Gewässerkunde. Band 1: Flußkunde [Compendium of hydrology]*. Göschen.

Hamad, R. (2020). Multiple morphometric characterization and analysis of Malakan valley drainage basin using GIS and remote sensing, Kurdistan Region, Iraq. *American Journal of Water Resources, 8*(1), 38–47. 10.12691/ajwr-8-1-5

Horton, R. E. (1945). Erosional development of streams and their drainage density: A hydrophysical approach to quantitative geomorphology. *Geological Society of America Bulletin, 56*, 275–370.

IPCC. (2021). Chapter 8: Water cycle changes. In *Climate change 2021: The physical science basis. Contribution of Working Group I to the Sixth Assessment Report of the Intergovernmental Panel on Climate Change*. Cambridge University Press. https://www.ipcc.ch/report/ar6/wg1/chapter/chapter-8/

Jakubínský, J., Bácová, R., Svobodová, E., Kubíček, P., & Herber, V. (2014). Small watershed management as a tool of flood risk prevention. *Proceedings of the International Association of Hydrological Sciences*, *364*, 243–248. https://doi.org/10.5194/PIAHS-364-243-2014

Jenson, S. K., & Domingue, J. O. (1988). Extracting topographic structure from digital elevation data for geographic information system analysis. *Photogrammetric Engineering and RemoteSensing, 54*(11), 1593–1600.

Jourgholami, M., Karami, S., Tavankar, F., Lo Monaco, A., & Picchio, R. (2020). Effects of slope gradient

on runoff and sediment yield on machine-induced compacted soil in temperate forests. *Forests, 12*(1), 49. https://doi.org/10.3390/f12010049

Lei, W., Dong, H., Chen, P., Lv, H., Fan, L., & Mei, G. (2020). Study on runoff and infiltration for expansive soil slopes in simulated rainfall. *Water, 12*(1), 222. https://doi.org/10.3390/w12010222

Mashauri, F., Mbuluyo, M., & Nkongolo, N. (2023). Influence des paramètres hydro-morphométriques sur l'écoulement des eaux des sous-bassins versants de la Tshopo, République Démocratique du Congo. *Revue Internationale de Géomatique, 32*, 79–98. https://doi.org/10.32604/RIG.2023.044124

Meddi, M., Talia, A., & Martin, C. (2009). Évolution récente des conditions climatiques et des écoulements sur le bassin versant de la Macta (Nord-Ouest de l'Algérie). *Physio-Géo. Géographie physique et environnement*, *3*, 61–84.

Merheb, M., Moussa, R., Abdallah, C., Colin, F., Perrin, C., & Baghdadi, N. (2016). Hydrological response characteristics of Mediterranean catchments at different time scales: A meta-analysis. *Hydrological Sciences Journal, 61*(14), 2520–2539. https://doi.org/10.1080/02626667.2016.1140174

Ministère des Forêts, de la Faune et des Parcs (MFFP), Québec. (2018). *Guide de réalisation d'aménagements durables en forêt privée – Annexe 6 : Méthodes de calcul des débits de pointe*. https://mffp.gouv.qc.ca

Nait-Si, H., Nmiss, M. H., Benbih, M., Boukdoun, A., & Ouammou, A. (2025). Impact des caractéristiques hydro-morphométriques sur la réponse hydrologique du bassin versant de l'oued Adoudou (Anti-Atlas occidental, Maroc) [Impact of hydro-morphometric characteristics on the hydrological response of the Oued Adoudou watershed (Western Anti-Atlas, Morocco)]. *Revista de Estudios Andaluces, 50*, 185–217. https://doi.org/10.12795/rea.2025.i50.09

Obeidat, M., Awawdeh, M., & Al-Hantouli, F. (2021). Morphometric analysis and prioritisation of watersheds for flood risk management in Wadi Easal Basin (WEB), Jordan, using geospatial technologies. *Journal of Flood Risk Management, 14*(2), e12711. https://doi.org/10.1111/jfr3.12711

Özcan, Z., Trinh, T., Kavvas, M. L., & Alp, E. (2025). Assessment of climate change for predicting water–energy–food–ecosystem nexus vulnerability in a semi-arid basin. *Journal of Water and Climate Change, 16*(2), 712–735. https://doi.org/10.2166/wcc.2024.703

Seethapathi, P. V., Dutta, D., & Kumar, R. S. (Eds.). (2008). *Hydrology of small watersheds*. TERI Press.

Shekar, P. R., & Mathew, A. (2024). Morphometric analysis of watersheds: A comprehensive review of data sources, quality, and geospatial techniques. *WatershedEcology and the Environment*, *6*, 13–25. https://doi.org/10.1016/j.wsee.2023.12.001

Strahler, A. N. (1957). Quantitative analysis of watershed geomorphology. *Transactions of the American Geophysical Union, 38*(6), 913–920. https://doi.org/10.1029/TR038i006p00913

Strahler, A. N. (1964). Quantitative geomorphology of drainage basins and channel networks. In V. T. Chow (Ed.), *Handbook of applied hydrology* (pp. 439–476). McGraw-Hill.

Topography Platform. (2023). *Données MNT 30m*. https://www.topography.com

Tramblay, Y., & Somot, S. (2018). Future evolution of extreme precipitation in the Mediterranean. *Climatic Change*, *151*(2), 289-302. https://doi.org/10.1007/s10584-018-2300-5

Vaze, J., & Teng, J. (2007). Impact of DEM resolution on topographic indices and hydrological modelling results. In *MODSIM 2007 International Congress on Modelling and Simulation*.

World Bank. (2020). *Adaptation to climate change in the Middle East and North Africa (MENA) region*. https://www.worldbank.org/en/topic/climatechange/publication/adaptation-to-climate-change-in-mena